[10]Bulirsch, R., "Die Mehrzielmethode zur numerischen Lösung von nichtlinearen Randwertproblemen and Aufgaben der optimalen Seuerung," Rept. of the Carl-Cranz-Gesellschaft, Oberpfaffenhofen, Germany, 1971.

[11]Oberle, H. J., "Numerische Berechnung optimaler Steuerungen von Heizung and Kühlung für ein realistisches Sonnenhausmodell," Institut für Mathematik der Technischen Universität München, TUM-M8310, Munich, Germany, 1983.

[12]Bock, R., "Numerische Behandlung von Zustandsbeschränkten und Chebychef-Steuerungsproblemen," Course R 1.06, Carl-Cranz-Gesellschaft, Oberpfaffenhofen, Germany, 1983.

[13]Brüning, G., Hafer, X., and Sachs, G., *Flugleistungen*, 2nd ed., Springer-Verlag, Berlin, 1986.

[14]Sachs, G., "Dynamic Decrease of Drag by Optimal Periodic Control," *Journal of Guidance, Control, and Dynamics*, Vol. 14, No. 4, 1991, pp. 860–863.

Performance of Higher Harmonic Control Algorithms for Helicopter Vibration Reduction

Steven R. Hall* and Norman M. Wereley†
Massachusetts Institute of Technology, Cambridge, Massachusetts 02139

I. Introduction

SIGNIFICANT vibration levels are encountered by helicopters because of variations in rotor blade aerodynamic loads with blade azimuth angle. These vibration levels reduce pilot effectiveness and passenger comfort and increase maintenance and operating costs. Thus, the control of helicopter rotors to reduce vibrations is of great interest.

Hooper[1] surveyed many major wind-tunnel and full-scale flight tests and determined that the primary cause of unsteady airloading above the second harmonic is the interaction of each rotor blade with the vortex of the preceding blade. The airloading of each blade is essentially periodic and can be decomposed as a sum of harmonics of the rotor frequency. For an N-bladed rotor, only vibrations at harmonics that are integer multiples of N times the rotor frequency are transmitted through the rotor mast, due to cancellation of the other harmonics by the N blades.

To reduce helicopter vibration, several methodologies known collectively as higher harmonic control (HHC) have been suggested. The basic idea behind HHC is to control rotor blades at harmonics of the rotor frequency so that unsteady airloads are canceled. One of the earliest HHC algorithms was suggested by Shaw,[2] with subsequent wind tunnel and flight tests.[3,4] In this approach, the control response matrix $\boldsymbol{T}$ is assumed to be known. The control response matrix relates the sine and cosine components of the N/rev swashplate inputs to the sine and cosine components of the N/rev response of the helicopter. At each step of the algorithm, a harmonic analysis of the measured quantity (either mast forces or accelerations at some fuselage location) is performed. The result is the sine and cosine components of the force (or acceleration) at the N/rev frequency. The vector of N/rev components is then multiplied by a decoupling matrix, which is the inverse of the control response matrix, to produce the change in commanded N/rev swashplate motion. Under the assumption that the control response of the helicopter to N/rev inputs is essentially quasisteady, this algorithm should eliminate N/rev vibrations in one step (that is, this method should produce deadbeat control).

Several authors[5–7] have proposed that stochastic adaptive controllers be used to account for parameter uncertainty and changing flight conditions. These methods are essentially derivative of Shaw's approach except that they include real-time identification of the control response matrix. The intent is to increase the robustness of the HHC algorithm to parameter uncertainty, changing flight conditions, and nonlinearities. However, this stochastic adaptive regulator implementation is much more complex than the fixed-gain controller advocated by Shaw. A review of these self-tuning regulators is provided by Johnson,[8] and some refinements are discussed by Davis.[9]

A different method, suggested by Gupta and DuVal[10] and DuVal et al.,[11] is the linear quadratic regulator with frequency-shaped cost functions, or LQR/FSCF. In this approach, the linear quadratic regulator is modified to allow for state and control penalties that are functions of frequency. By placing an infinite weight on the N/rev response, a controller is developed that is guaranteed to drive the N/rev response to zero.

A number of HHC algorithms have been the subject of wind-tunnel tests[3,12–15] and flight tests.[16–20] These tests have generally shown reductions in vibration levels of 25–90%. Shaw et al.[21] tested fixed-gain, gain-scheduled, and adaptive regulators on a dynamically scaled model of the three-bladed CH-47D Chinook rotor. This study showed that the fixed-gain regulator was 90% effective in suppressing three vibration components in almost all of the trimmed and quasisteady maneuvering envelope. Shaw also determined that a gain-scheduled controller provided no additional benefits over the fixed-gain controller. In testing two types of adaptive controllers, namely, global and local versions, the global controller was found to be unstable and the local controller was successful to the same extent as the fixed-gain regulator. Therefore, the fixed-gain regulator appears to be sufficient for eliminating most vibrations, and gain scheduling and/or adaptation of the $\boldsymbol{T}$ matrix is not of crucial importance.

In this Note, a framework is provided for the evaluation of HHC algorithm performance in terms of classical control theory. Single input/single output (SISO) characterizations of HHC algorithms are used to develop insight into the HHC problem. It is shown that HHC is fundamentally similar to the sinusoidal disturbance rejection techniques of classical control. By treating the periodic disturbance as a stochastic rather than a deterministic phenomenon, the performance of different HHC algorithms can be compared quantitatively. Furthermore, this framework allows the direct comparison of the discrete-time algorithms of Shaw and others to continuous-time algorithms, such as those of Gupta and DuVal.[10] Finally, this framework allows the investigation of the effects of model uncertainty due to parameter uncertainty and changing flight conditions.

II. Quasisteady Approach

Many authors, including Shaw et al.,[3,4,13,21,22] McCloud,[23–25] Wood et al.,[19] and Molusis,[5,6] represent the dynamic response of a helicopter to control inputs at the N/rev frequency by a constant matrix $\boldsymbol{T}$ that relates the Fourier coefficients of the N/rev harmonics of the swashplate commands to the N/rev harmonics of the vibration. This approach eliminates the need for a detailed model of the periodic helicopter dynamics, but requires that the controller bandwidth be low enough that the dynamics of the helicopter can be treated as quasisteady. In this section it will be demonstrated that the algorithm proposed by Shaw (and similar algorithms) behave similarly to the

Received June 14, 1991; revision received April 30, 1992; accepted for publication July 24, 1992.

*Associate Professor, Department of Aeronautics and Astronautics. Senior Member AIAA.

†Research Assistant, Department of Aeronautics and Astronautics; currently, Staff Member, BDM International, Inc., Arlington, VA 22203. Member AIAA.

classical continuous-time compensators designed for rejection of narrowband disturbances.

Using the quasisteady assumption, the sine and cosine components of the N/rev vibration may be represented by

$$z = Tu + z_0 \tag{1}$$

where z is a vector of vibration amplitudes, u the vector of N/rev swashplate amplitudes, and z_0 the vector of vibration amplitudes for zero swashplate deflection. That is, z_0 is the uncontrolled disturbance to be rejected. Shaw's algorithm is based on canceling the disturbance z_0 by use of the swashplate inputs u. Since the disturbance input z_0 is unknown a priori, the approach taken is to measure the vibration level at each time step and adjust the swashplate input u to cancel the measured disturbance. The resulting control law is

$$u_{n+1} = u_n - T^{-1} z_n \tag{2}$$

where the subscripts denote the index of the time step. For periodic disturbances, this control law is deadbeat and should completely reject the disturbance in one controller time period.

A block diagram of the discrete-time implementation of Shaw's algorithm is shown in Fig. 1. The forward loop consists of the static plant model T, where a disturbance waveform $d(t)$ is added to the plant output to obtain the vibration $z(t)$. The vibration measurement z_n is obtained by a Fourier decomposition of the vibration at the N/rev frequency. First, the signal $z(t)$ is multiplied by sine and cosine signals to demodulate it. The time-varying sine and cosine components are then integrated over one time period to obtain the sine and cosine components of the vibration z_{s_n} and z_{c_n}. These components are multiplied by the inverted plant T^{-1} to obtain the appropriate control adjustment Δu_{s_n} and Δu_{c_n}. These signals are then added to the previous control to obtain the next control commands $\Delta u_{s_{n+1}}$ and $\Delta u_{c_{n+1}}$. Finally, the swashplate command is obtained by modulating $\Delta u_{s_{n+1}}$ and $\Delta u_{c_{n+1}}$ by sin $N\Omega t$ and cos $N\Omega t$, respectively.

It can be shown[26] that the block diagram of Fig. 1 can be simplified by replacing the integration over one time period by a continuous integration and by replacing the delay and summation by a sample-and-hold to obtain $\Delta u_{s_{n+1}}$ and $\Delta u_{c_{n+1}}$.

Continuous-time Algorithm: A fairly obvious way to obtain a continuous-time HHC algorithm is to eliminate the sample-and-hold just described in favor of a direct connection. The resulting continuous-time algorithm is useful for understanding the behavior and performance of HHC algorithms based on the quasisteady assumption. In this Note we concentrate on the continuous-time algorithm; however, most of the results apply to the discrete-time case as well.

At this point it is instructive to consider how the continuous version of Shaw's algorithm applies to a helicopter whose swashplate-to-vibration dynamics can be represented by a SISO, linear time-invariant (LTI) transfer function $\hat{G}(s)$. In this case, T is given by

$$T = \begin{bmatrix} T_{cc} & T_{cs} \\ T_{sc} & T_{ss} \end{bmatrix} \tag{3}$$

where

$$T_{cc} = T_{ss} = \mathrm{Re}\{\hat{G}(jN\Omega)\}, \qquad T_{cs} = -T_{sc} = \mathrm{Im}\{\hat{G}(jN\Omega)\} \tag{4}$$

(The symmetry that results in T is often approximately satisfied for actual helicopters, although the plant is obviously not time invariant.) The HHC compensator in continuous time $\hat{H}(s)$ that results can be shown[26] to be

$$\hat{H}(s) = -\frac{\hat{u}(s)}{\hat{z}(s)} = \frac{2k(as + bN\Omega)}{s^2 + (N\Omega)^2} \tag{5}$$

where

$$a = \mathrm{Re}\{\hat{G}(jN\Omega)\}/|\hat{G}(jN\Omega)|^2$$
$$b = \mathrm{Im}\{\hat{G}(jN\Omega)\}/|\hat{G}(jN\Omega)|^2 \tag{6}$$
$$k = 1/T$$

Note that $\hat{H}(s)$ is infinite at $s = \pm jN\Omega$, so that the sensitivity transfer function $\hat{S}(s)$, which is the ratio of the closed-loop vibration level to the open-loop vibration level, is zero at $s = \pm jN\Omega$. That is, if the vibration is truly periodic, then the preceding compensator should completely eliminate the vibration. This disturbance rejection property results from the poles at $s = \pm jN\Omega$ in $\hat{H}(s)$ and not from an exact knowledge of the matrix T. Therefore, a compensator of the form of Eq. (5) will completely eliminate the N/rev harmonics of the vibrations if the vibration is periodic and the closed-loop system is stable. This result holds for the discrete-time compensator as well. Note, however, that the deadbeat behavior of the discrete-time algorithm will be lost if the matrix T is mismodeled. This has important implications for adaptive control, as will be shown in the sequel.

The closed-loop stability of the compensator may be determined using root locus techniques. In particular, consider the compensator pole at $s = jN\Omega$. The residue of this pole is given by

$$\mathrm{Res}\left[\hat{G}(s)\hat{H}(s);\ s = jN\Omega\right] = 2k\hat{G}(s)\frac{as + bN\Omega}{s + jN\Omega}\bigg|_{s=jN\Omega} = k = \frac{1}{T} \tag{7}$$

Therefore, it can be concluded that 1) the angle of departure of the compensator poles, which depends on the zero location determined by a and b, is 180 deg, so that the closed-loop poles move into the left half-plane (that is, the poles are stabilized); and 2) to first order in k, the closed-loop poles are $s = \pm jN\Omega - k = \pm jN\Omega - 1/T$. Since the real part of the closed-loop poles are $s = -1/T$, the settling time of the closed-loop system is T. These results also demonstrate the importance of the quasisteady assumption. If the settling time of the plant dynamics is not short compared with T, then there may be poles that are driven unstable by the introduction of feedback.

The residue k plays much the same role for the rejection of periodic (or narrowband) disturbances as the velocity error constant plays for the rejection of constant (or low frequency) disturbances. (Recall that the velocity error constant is simply the residue of the pole at $s = 0$ of a type 1 system.) Said another way, k is the velocity error constant of the HHC control system if we consider the (demodulated) sine and cosine components of the vibration to be constant or slowly varying disturbances to be eliminated. In the sequel we will

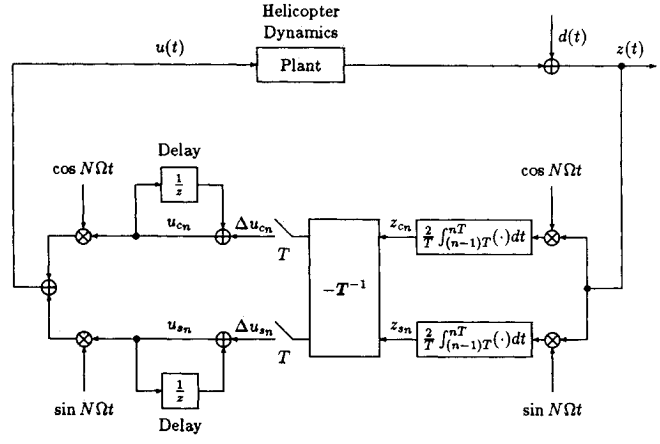

Fig. 1 Block diagram of the discrete-time higher harmonic control algorithm.

refer to k as the "velocity constant" of the system, although this is a slight abuse of nomenclature.

In summary, the more complicated modulation-demodulation structure of Shaw's HHC compensator can be reduced, in continuous time, to the classical LTI feedback compensation structure that might be used for narrowband disturbance rejection of a known periodic signal. In the sequel, the continuous-time HHC algorithm will be used to illustrate some fundamental limitations on HHC performance. In addition, it will be shown that the continuous-time algorithm has some performance advantages over the discrete-time algorithm.

III. Frequency-Shaped Cost Functions

The periodicity of the rotor flowfield produces periodic disturbances and makes the dynamics of the rotor periodic. The latter effect is less important, and an LTI dynamic model of the helicopter often may be used. The LTI assumption allows the use of a host of multivariable control design techniques. An approach that has been applied to the active control of helicopter vibrations by Gupta and Du Val[10] and Du Val et al.[11] is the LQR/FSCF described below.

The LTI assumption allows the transfer function $\hat{G}(s)$ to be represented by a state-space model of the form

$$\dot{x}_p(t) = A_p x_p(t) + B_p u(t) \tag{8}$$

$$z(t) = C_p x_p(t) + d(t) \tag{9}$$

where $x_p(t)$ is the vector of helicopter plant states, $u(t)$ the swashplate command, $d(t)$ the disturbance, and $z(t)$ the vibration output. In the LQR/FSCF approach, the state feedback gains are found that minimize the frequency-based cost function proposed by Gupta[27]

$$J = \int_{-\infty}^{\infty} \left\{ z^H(j\omega) Q_{zz}(\omega) z(j\omega) + \rho u^H(j\omega) u(j\omega) \right\} d\omega \tag{10}$$

where the superscript H denotes the complex conjugate transpose. To eliminate vibrations at the N/rev frequency, the weighting function $Q_{zz}(\omega)$ must be large at the N/rev frequency. The frequency shaping is accomplished by appending a filter to the vibration measurement that is tuned to resonate at the N/rev frequency, namely,

$$\hat{G}_N(s) = \frac{(N\Omega)^2 s}{s^2 + (N\Omega)^2} \tag{11}$$

The frequency-shaped cost function can be transformed to a time domain LQR problem by adjoining the filter states x_N to the plant states x_p to form the augmented state vector x. The solution of the LQR problem yields a matrix of optimal feedback gains F, where the control law is of the form

$$u(t) = -Fx(t) \tag{12}$$

The closed-loop optimal regulator poles are the stable roots of the symmetric roots characteristic equation[28]

$$1 + (1/\rho)\hat{G}(s)\hat{G}_N(s)\hat{G}_N(-s)\hat{G}(-s) = 0 \tag{13}$$

Equation (13) is in the form of a root locus equation with a double pole at $s = \pm jN\Omega$. Therefore, for large ρ, the asymptotic pole locations near $s = jN\Omega$ are governed by

$$1 - (1/4\rho)\hat{G}(jN\Omega)\hat{G}(-jN\Omega)\{(N\Omega)^4/[(s - jN\Omega)^2]\} = 0 \tag{14}$$

so that the closed-loop regulator poles are at

$$s \approx \pm jN\Omega - (1/2\sqrt{\rho})\,|\hat{G}(jN\Omega)|\,(N\Omega)^2 \tag{15}$$

That is, the closed-loop poles are located immediately left of $s = \pm jN\Omega$ in the s plane. This result is similar to that found in Sec. II, where the closed-loop poles were found to be at $s = \pm jN\Omega - k$.

Furthermore, Gupta and DuVal[10] demonstrated that the vibration controller need not implement full state feedback of rotor, fuselage, and filter states to achieve good performance. The elimination of fuselage state feedback does not significantly alter closed-loop pole locations if rotor state feedback is maintained. In addition, due to the complexity of estimating rotor states, a vibration controller that only feeds back the filter states $x_N(t)$ is desirable. Gupta and DuVal anticipated that rotor state feedback could also be eliminated if a low-pass filter were implemented on the roll rate feedback of the stability augmentation system (SAS) to prevent low-frequency rotor modes from driving the SAS unstable in roll. Hence, a simplified representation of the LQR/FSCF compensator for N/rev disturbance rejection is of the form

$$\hat{H}(s) = \frac{(F_1 + F_2 s)(N\Omega)^2}{s^2 + (N\Omega)^2} \tag{16}$$

This compensator has the same form as Eq. (5), that is, the compensator has a single real zero and poles at $s = \pm jN\Omega$. Furthermore, the zero in this compensator is at nearly the same location as the zero in Eq. (5).

Thus, the quasisteady approach (using the continuous-time equivalent compensator) and the LQR/FSCF approach produce similar results, except perhaps for the velocity constant k, which is governed here by the choice of ρ in the cost function. Therefore, we will consider only the compensator of Eq. (5) in the remainder of this Note, with the understanding that the LQR/FSCF approach will give similar performance.

IV. Response to Disturbances

In Sec. II it was argued that HHC algorithms should completely eliminate periodic vibration. In practice, HHC algorithms reject only 25 to 90% of the N/rev vibration. Here we explore some of the possible explanations for this result.

One reason that has been advanced for incomplete rejection of N/rev vibration is the lack of knowledge of the true T matrix. This has led a number of investigators[5-7] to develop adaptive HHC algorithms that estimate T in real time. However, the arguments of Sec. II demonstrate that it is the integral action of the compensator that produces complete disturbance rejection. Exact knowledge of T is required only if deadbeat behavior is required.

Similarly, nonlinear behavior of the helicopter has been proposed as a possible mechanism causing incomplete disturbance rejection.[6] If the plant dynamics are nonlinear, two types of stable closed-loop behavior are possible: 1) the system may reach a periodic equilibrium trajectory, driven by the periodic disturbance, and 2) the system may be chaotic. In the first case, the integral action of the compensator will still lead to zero steady-state vibration at the N/rev harmonic. In the second case, adaptation of T is unlikely to lead to improved performance.

One possibility that has not been widely considered in the HHC literature is that the disturbance may be random rather than deterministic. The randomness may be produced by atmospheric turbulence, instability of the vortices in the rotor wake, maneuvering, etc. Chaotic behavior may also be treated as random. (There is, in fact, some evidence of chaotic behavior in helicopter vibration.[29]) Whatever the mechanism, randomness of the vibration will certainly increase the closed-loop vibration level. Below, we quantify that increase in terms of the open-loop vibration spectrum.

A realistic approach is to model the harmonic disturbance as a random process with power spectral density centered about the N/rev frequency. Using this approach, quantitative comparisons can be made between alternative HHC algorithms in terms of the rms vibration levels that remain after closing the loop. The mechanism that produces the randomness may be characterized by its correlation time τ. The corre-

lation time τ may be the time constant of the turbulence, the average time between maneuvers, or any other constant that reflects the time scale over which the disturbance changes. Therefore, the width or spread of the disturbance spectrum is characterized by the inverse of the correlation time, or $1/\tau$.

The exact level of attenuation of the N/rev vibration (in an rms sense) depends on the form of the disturbance spectrum. Analytically tractable forms include a random walk model and a Gauss-Markov model. However, it turns out that the attenuation achieved is nearly independent of the form chosen for the spectrum. Hall and Wereley[26] show that

$$\sigma_z/\sigma_d \approx 1/\sqrt{k\tau} = \sqrt{T/\tau} \tag{17}$$

where σ_z and σ_d are the closed-loop and open-loop rms vibration levels, respectively. As would be expected, the attenuation improves as the correlation time or the velocity constant is increased.

The results of this section demonstrate the importance of the velocity constant k in determining closed-loop HHC performance. In particular, note that even for large values of $k\tau$, the disturbance attenuation may not be as large as desired. For example, even if the correlation time is as large as $\tau = 25T$ (i.e., 25 or 50 rotor revolutions), the closed-loop vibration level will be 20% of the open-loop vibration level.

In the discrete-time case, it is not possible to compute a transfer function for the closed-loop system as in the continuous-time case. However, the rms vibration levels can be propagated numerically. This procedure is described in detail in Ref. 26 and is omitted here for the sake of brevity. The rms vibration level asymptotically approaches

$$\sigma_z/\sigma_d \approx \sqrt{5/3}/\sqrt{k\tau} = 1.291/\sqrt{k\tau} \tag{18}$$

which is similar to the continuous-time case. The vibration level is slightly higher (29%) in the discrete-time case than for the equivalent continuous-time HHC controller, suggesting that a modest improvement in performance may be gained by using the continuous algorithm. The poorer performance of the discrete-time algorithm results from the fact that it uses old information (from the previous period) to determine the swashplate command, whereas the continuous-time algorithm uses current information.

V. Sensitivity to Modeling Error

The deadbeat behavior of the discrete-time algorithm discussed in Sec. II depends critically on knowledge of the matrix $\boldsymbol{T}$. In practical applications there will always be some modeling error so that deadbeat disturbance rejection will not occur. Variations in $\boldsymbol{T}$ may be due to changes in flight condition, maneuvering, etc. Also, it may be difficult to accurately estimate $\boldsymbol{T}$ from wind-tunnel or flight test data. In this section we quantify the stability robustness and performance robustness of HHC algorithms.

Stability Robustness

Our first concern is whether an HHC algorithm is stable in the face of modeling errors. The stability of the HHC algorithms discussed in this Note depends on phase stabilization near the frequency $\omega = N\Omega$ and gain stabilization everywhere else. Gain stabilization away from $\omega = N\Omega$ is achieved when the quasisteady assumption is approximately satisfied, as is generally the case. Phase stabilization is achieved near $\omega = N\Omega$ because the phase of the HHC compensator is adjusted so that the residue of the pole at $s = jN\Omega$ is k, a real, positive number. This implies that the phase margin in the vicinity of $\omega = N\Omega$ is ± 90 deg. Therefore, we conclude that the continuous-time HHC algorithm is quite robust, with large gain and phase margins.

In the discrete-time case, it can be shown[26] that the gain margin is 2 and the phase margin is ± 60 deg, assuming that the quasisteady assumption is valid. Although not as large as those in the continuous-time case, these stability margins are quite good, and we conclude that both the continuous-time and discrete-time HHC algorithms are quite robust.

Performance Robustness

Even if an HHC algorithm is stable, its performance may be degraded by variations in $\boldsymbol{T}$. To quantify the effects of modeling error on HHC performance, the results of Sec. IV can be extended to include errors in the control response matrix $\boldsymbol{T}$. Following the framework of Sec. II, we assume that the modeling error can be represented as a multiplicative error, so that

$$\boldsymbol{T} = \boldsymbol{E}\boldsymbol{T}_0 \tag{19}$$

where $\boldsymbol{T}_0$ is the modeled control response matrix and $\boldsymbol{T}$ the actual control response matrix. The multiplicative error is of the form

$$\boldsymbol{E} = \begin{bmatrix} e_1 & e_2 \\ -e_2 & e_1 \end{bmatrix} \tag{20}$$

Note that e_1 and e_2 correspond to the real and imaginary parts of the error, respectively. In general, arbitrary choices for all four elements should be permitted, but for the present development the preceding symmetric form is sufficient.

For a disturbance with correlation time τ, the rms attenuation of the vibration level is given by[26]

$$\sigma_z/\sigma_d \approx 1/\sqrt{ke_1\tau} \tag{21}$$

This result is similar to that determined earlier, that is, the mean-square vibration level is inversely proportional to the product of the real part of the velocity constant and the correlation time. Therefore, moderate modeling errors will not reduce the closed-loop performance by much. For example, a 45-deg phase error in estimating the helicopter response will increase the closed-loop rms vibration level by only about 19%. Thus, the performance of the continuous-time HHC algorithm is quite robust with respect to modeling errors. In the discrete-time case the situation is more complicated, but it can be shown[26] that the rms vibration level is not very sensitive to the multiplicative errors, within reasonable limits, although the discrete-time algorithm is not as robust as the continuous-time algorithm. The performance robustness of HHC algorithms explains to a large extent the success of the fixed-gain controllers in wind-tunnel tests.[21]

VI. Conclusions

Helicopter vibration suppression using higher harmonic control has been discussed in the context of classical linear control theory. Most HHC algorithms may be interpreted as classical, narrowband disturbance rejection compensators. It is the integral action of these compensators, not detailed knowledge of the helicopter dynamics, that is responsible for the disturbance rejection achieved by HHC algorithms. This integral action may be embedded in the harmonic analysis of the discrete-time algorithms, or it may be explicit in the denominator of the compensator transfer function. For this reason, adaptation is not likely to improve the performance of HHC algorithms significantly. One explanation for incomplete disturbance rejection in current HHC algorithms is that the disturbance is random, not deterministic. As such, the velocity constant of the HHC compensator and the correlation time of the disturbance both play a major role in determining HHC performance. Finally, implementation of HHC in continuous-time rather than discrete-time may produce significant improvements in gain and phase margin and modest improvements in performance.

Acknowledgment

The authors gratefully acknowledge the support of Boeing Helicopters for this work.

References

[1]Hooper, W. E., "The Vibratory Airloading of Helicopter Rotors," *Vertica,* Vol. 8, No. 2, 1984, pp. 73-92.

[2]Shaw, J., "A Feasibility Study of Helicopter Vibration Reduction by Self-Optimizing Higher Harmonic Blade Pitch Control," M.S. Thesis, Dept. of Aeronautics and Astronautics, Massachusetts Inst. of Technology, Cambridge, MA, 1967.

[3]McHugh, F. J., and Shaw, J., "Helicopter Vibration Reduction with Higher Harmonic Blade Pitch," *Journal of the American Helicopter Society,* Vol. 23, No. 4, 1978, pp. 26-35.

[4]Shaw, J., and Albion, N., "Active Control of Rotor Blade Pitch for Vibration Reduction: A Wind Tunnel Demonstration," *Vertica,* Vol. 4, No. 1, 1980, pp. 3-11.

[5]Molusis, J. A., Hammond, C. E., and Cline, J. H., "A Unified Approach to the Optimal Design of Adaptive and Gain Scheduled Controllers to Achieve Minimum Helicopter Rotor Vibration," *Journal of the American Helicopter Society,* Vol. 28, No. 2, 1983, pp. 9-18.

[6]Molusis, J. A., "The Importance of Nonlinearity in the Higher Harmonic Control of Helicopter Vibration," American Helicopter Society, Alexandria, VA, 1983, pp. 624-647.

[7]O'Leary, J., and Miao, W., "Design of Higher Harmonic Control for the ABC," *Journal of the American Helicopter Society,* Vol. 27, No. 1, 1982, pp. 52-57.

[8]Johnson, W., "Self-Tuning Regulators for Multicyclic Control of Helicopter Vibration," NASA TP-1996, March 1982.

[9]Davis, M. W., "Refinement and Evaluation of Helicopter Real-Time Self-Adaptive Active Vibration Controller Algorithms," NASA CR-3821, Aug. 1984.

[10]Gupta, N. K., and Du Val, R. W., "A New Approach for Active Control of Rotorcraft Vibration," *Journal of Guidance and Control,* Vol. 5, No. 2, 1982, pp. 143-150.

[11]Du Val, R. W., Gregory, C. Z., Jr., and Gupta, N. K., "Design and Evaluation of a State-Feedback Vibration Controller," *Journal of the American Helicopter Society,* Vol. 29, No. 3, 1984, pp. 30-37.

[12]McKillip, R. M., Jr., "Periodic Control of the Individual-Blade-Control Helicopter Rotor," *Vertica,* Vol. 9, No. 2, 1985, pp. 199-225.

[13]Shaw, J., and Albion, N., "Active Control of the Helicopter Rotor for Vibration Reduction," *Journal of the American Helicopter Society,* Vol. 26, No. 3, 1981, pp. 32-39.

[14]Hammond, C. E., "Wind Tunnel Results Showing Rotor Vibratory Loads Reduction Using Higher Harmonic Blade Pitch," *Journal of the American Helicopter Society,* Vol. 28, No. 1, 1983, pp. 10-15.

[15]Lehmann, G., "A Digital System for Higher Harmonic Control of a Model Rotor," *Vertica,* Vol. 8, No. 2, 1984, pp. 165-181.

[16]Miao, W., Kottapalli, S. B. R., and Frye, H. M., "Flight Demonstration of Higher Harmonic Control (HHC) on S-76," *Proceedings of the 42nd Annual Forum of the American Helicopter Society,* American Helicopter Society, Alexandria, VA, 1986, pp. 777-791.

[17]O'Leary, J., Kottapalli, S. B. R., and Davis, M., "Adaptation of a Modern Medium Helicopter (Sikorsky S-76) to Higher Harmonic Control," *Proceedings of the 2nd Decennial Specialists Meeting on Rotorcraft Dynamics*, American Helicopter Society, Alexandria, VA, Nov. 1984, Paper No. 23.

[18]Walsh, D. M., "Flight Tests of an Open Loop Higher Harmonic Control System on an S-76A Helicopter," *Proceedings of the 42nd Annual Forum of the American Helicopter Society,* American Helicopter Society, Alexandria, VA, 1986, pp. 831-843.

[19]Wood, E. R., Powers, R. W., Cline, J. H., and Hammond, C. E., "On Developing and Flight Testing a Higher Harmonic Control System," *Journal of the American Helicopter Society,* Vol. 30, No. 1, 1985, pp. 3-20.

[20]Polychroniadis, M., and Achache, M., "Higher Harmonic Control: Flight Tests of an Experimental System on SA 349 Research Gazelle," *Proceedings of the 42nd Annual Forum of the American Helicopter Society,* American Helicopter Society, Alexandria, VA, 1986, pp. 811-820.

[21]Shaw, J., Albion, N., Hanker, E. J., Jr., and Teal, R. S., "Higher Harmonic Control: Wind Tunnel Demonstration of Fully Effective Vibratory Hub Force Suppression," *Journal of the American Helicopter Society,* Vol. 34, No. 1, 1989, pp. 14-25.

[22]Shaw, J., "Higher Harmonic Blade Pitch Control: A System for Helicopter Vibration Reduction," Ph.D. Thesis, Dept. of Aeronautics and Astronautics, Massachusetts Inst. of Technology, Cambridge, MA, 1980.

[23]McCloud, J. L., III, "The Promise of Multicyclic Control," *Vertica,* Vol. 4, No. 1, 1980, pp. 29-41.

[24]McCloud, J. L., III, and Weisbrich, A. L., "Wind-Tunnel Results of a Full-Scale Multicyclic Controllable Twist Rotor," *Proceedings of the 34th Annual Forum of the American Helicopter Society,* American Helicopter Society, Alexandria, VA, 1978 (Paper No. 78-60).

[25]McCloud, J. L., III, "An Analytical Study of a Multicyclic Controllable Twist Rotor," *Proceedings of the 31st Annual Forum of the American Helicopter Society,* American Helicopter Society, Alexandria, VA, 1975 (Paper No. 932).

[26]Hall, S. R., and Wereley, N. M., "Linear Control Issues in the Higher Harmonic Control of Helicopter Vibrations," *Proceedings of the 45th Annual Forum of the American Helicopter Society,* American Helicopter Society, Alexandria, VA, 1989, pp. 955-972.

[27]Gupta, N. K., "Frequency-Shaped Cost Functionals: Extension of Linear-Quadratic-Guassian Design Method," *Journal of Guidance and Control,* Vol. 3, No. 6, 1980, pp. 529-535.

[28]Kwakernaak, H., and Sivan, R., *Linear Optimal Control Systems,* Wiley, New York, 1972, pp. 281-296.

[29]Sarigul-Klijn, M. M., Kolar, R., Wood, E. R., and Straub, F. K., "On Chaos Methods Applied to Higher Harmonic Control," *Proceedings of the 46th Annual Forum of the American Helicopter Society,* American Helicopter Society, Alexandria, VA, 1990, pp. 79-98.

Autonomous Position and Velocity Determination in Interplanetary Space

John D. Vedder*
McDonnell Douglas Space Systems Company, Houston, Texas 77062

Introduction

THE purpose of this Note is to describe briefly a new method for autonomously estimating the position and velocity state vector of an interplanetary spacecraft. This method is based solely on a small number of sequential, time-tagged sightings of known objects with onboard optical equipment. These objects consist of the planets or their satellites and the brighter asteroids. The only qualifications for these objects are that they must be observable with onboard instrumentation, such as a star tracker; their ephemerides must be known onboard; and they must not be pairwise coplanar with the spacecraft's trajectory during the observation interval.

It is known that *simultaneous* sightings of two such objects against their stellar backgrounds can be used to determine the observer's position in interplanetary space, and detailed analyses of this process are available.[1,2] However, this process has some important limitations, including the following: sightings should ideally be simultaneous, necessitating multiple instruments and observers; no *direct* information about velocity is obtained; and any error in either of the two sightings will have a large effect on the result. Geometrically, this method fixes the observer's position as the point determined by the intersection of two straight lines in space.

The new method proposed here requires four *sequential*, time-tagged sightings of such objects to determine four lines in space. The direction of each line is extracted from the object's location against its observed stellar background. Knowing both this direction vector and the object's location (from its known ephemeris) defines the straight line in space. The observer's trajectory during the sighting interval is then approximated by the straight line that intersects each of the four known lines; actually two such solutions exist,[3] one represent-

Received June 30, 1992; presented as Paper 92-4599 at the AIAA Guidance, Navigation, and Control Conference, Hilton Head, SC, Aug. 10-12, 1992; revision received Sept. 1, 1992; accepted for publication Sept. 14, 1992.

*Specialist, Houston Division, 16055 Space Center Boulevard; currently Independent Consultant. Senior Member AIAA.